Received: 14 July 2022 | Revised: 3 April 2023 | Accepted: 6 April 2023

DOI: 10.1111/cas.15820

Cancer Science WILEY

ORIGINAL ARTICLE

Circular RNA circARHGEF28 inhibited the progression of prostate cancer via the miR-671-5p/LGALS3BP/NF-κB axis

Kaixuan Guo[1,2,3] | Juanyi Shi[2,4] | Zhuang Tang[1,2,3] | Cong Lai[1,2,3] | Cheng Liu[1,2,3] | Kuiqing Li[1,2,3] | Zhuohang Li[1,2,3] | Kewei Xu[1,2,3]

[1]Department of Urology, Sun Yat-sen Memorial Hospital, Sun Yat-sen University, Guangzhou, China

[2]Guangdong Provincial Key Laboratory of Malignant Tumor Epigenetics and Gene Regulation, Sun Yat-sen Memorial Hospital, Sun Yat-sen University, Guangzhou, China

[3]Guangdong Provincial Clinical Research Center for Urological Diseases, Guangzhou, China

[4]Department of Hepatobiliary Surgery, Sun Yat-Sen Memorial Hospital, Sun Yat-Sen University, Guangzhou, China

Correspondence
Kewei Xu, 107th Yanjiangxi Road, Guangzhou, GD 510120, China.
Email: xukewei@mail.sysu.edu.cn

Funding information
Guangdong Basic and Applied Basic Research Foundation, Grant/Award Number: 2021A1515010199; Guangdong Provincial Clinical Research Center for Urological Diseases, Grant/Award Number: 2020B1111170006; Guangdong Science and Technology Department, Grant/Award Number: 2020B1212060018; Key Areas Research and Development Program of Guangdong, Grant/Award Number: 2020B111114002; Medical Science and Technology Research Foundation of Guangdong Province, Grant/Award Number: A2022541; Medical Scientific Research Foundation of Guangdong Province, Grant/Award Number: C2018060; National Natural Science Foundation of China, Grant/Award Number: 82072841; the Science and Technology Program of Guangzhou, Grant/Award Number: 201803010029 and 202011020004; Yixian Clinical Research Project of Sun Yat-sen Memorial Hospital, Grant/Award Number: SYS-C-201802

Abstract

Circular RNAs (circRNAs) play crucial roles in various biological processes, including prostate cancer (PCa). However, the precise roles and mechanism of circRNAs are complicated. Hence, we studied the function of a circRNA that might be involved in the progression of PCa. In this study, we found that circARHGEF28 was frequently downregulated in PCa tissues and cell lines. Furthermore, gain- and loss-of function experiments in vitro showed that circARHGEF28 inhibited proliferation, migration, and invasion of PCa. Additionally, circARHGEF28 suppressed PCa progression in vivo. Bioinformatics analysis and RNA pull-down and capture assay found that circARHGEF28 sponged miR-671-5p in PCa cells. Importantly, qRT-PCR and dual luciferase assays found that Lectin galactoside-binding soluble 3 binding protein (LGALS3BP) was downstream of miR-671-5p, and western blot analysis further confirmed that LGALS3BP negatively regulated the nuclear factor kappa-B (NF-κB) pathway. These results demonstrated that circARHGEF28 abolished the degradation of LGALS3BP by sponging miR-671-5p, thus blocking the activation of the NF-κB pathway. Our findings revealed that circARHGEF28/miR-671-5p/LGALS3BP/NF-κB may be an important axis that regulates PCa progression.

KEYWORDS
circARHGEF28, LGALS3BP, miR-671-5p, NF-κB, prostate cancer

Abbreviations: CCK-8, Cell Counting Kit-8; cDNA, complementary DNA; circRNAs, circular RNAs; CRPC, castration-resistant prostate cancer; FBS, fetal bovine serum; HE, hematoxylin and eosin staining; LGALS3BP, Lectin galactoside-binding soluble 3 binding protein; NF-κB, nuclear factor kappa-B; PCa, prostate cancer; qRT-PCR, quantitative real-time PCR; siRNA, small interfering RNA.

Kaixuan Guo, Juanyi Shi and Zhuang Tang contributed equally to this work.

1 | INTRODUCTION

Prostate cancer (PCa) is the most common type of malignant tumor of the urinary system and the second leading cause of cancer-related deaths in males worldwide.[1] Despite great improvements in prostatectomy and endocrine therapy, the prognosis is highly heterogeneous.[2] It is inevitable that hormone-sensitive PCa eventually progresses to castration-resistant prostate cancer (CRPC) even after aggressive treatment.[3] Unfortunately, approximately 30% of CRPC cases develop distant metastasis, which dramatically reduces the overall survival of PCa patients.[4–6] The vague understanding of the pathogenesis of PCa seriously restricts the effectiveness of treatment. Hence, it is vital to explore potential therapeutic targets and clarify the molecular mechanisms in PCa.

Circular RNAs (circRNAs) represent a novel class of noncoding RNAs lacking a 5′ cap and a 3′ polyadenylated tail.[7] They are characterized by a covalently closed loop through the reverse splicing of pre-mRNA transcripts.[8] Unlike linear messenger RNAs (mRNAs), circRNAs can stably exist in specific tissues and cell lines.[9] Abundant dysregulated circRNAs have been identified in various cancers, indicating that circRNAs may participate in tumor-related biological processes. Growing evidence indicates that circRNAs play a critical role in prostate,[10] lung,[11] breast,[12] colorectal,[13] and bladder cancers.[14] Mechanistically, although several studies have summarized that circRNAs function as microRNA (miRNA) sponges, RNA-binding proteins, and encoding polypeptides in tumor progression,[15–17] the relationship between circRNAs and PCa progression remains elusive.

In the present study, a circRNA molecule generated from exon 11 of ARHGEF28 (circARHGEF28) was identified successfully, and the function was determined in the PCa. We found that circARHGEF28 was frequently downregulated in PCa tissues, implying its potential negative association with PCa. Functional experiments suggested that circARHGEF28 inhibited the malignant phenotype of PCa in vitro and in vivo. Mechanistically, we revealed that circARHGEF28 sponged miR-671-5p to elevate LGALS3BP expression and subsequently inactivated the nuclear factor kappa-B (NF-κB) pathway, restraining PCa progression eventually. Collectively, our results revealed that the circARHGEF28/miR-671-5p/LGALS3BP/NF-κB axis played a crucial role in PCa progression.

2 | MATERIALS AND METHODS

2.1 | Clinical tumor samples

PCa tissues and paired normal prostate tissues were collected from patients who underwent radical resection surgery at Sun Yat-sen Memorial Hospital, Sun Yat-sen University (Guangzhou, China). All clinical samples were diagnosed with PCa after pathological diagnosis and stored at −80°C with RNALater immediately after acquisition. This study was approved by the Ethical Review Committee of Sun Yat-sen Memorial Hospital and an informed consent form for each patient was signed before collecting samples.

2.2 | Cell lines, culture, and treatments

The human PCa cell lines PC-3, DU145, LNCap, and 22Rv1 and the immortalized normal uroepithelium cell line (RWPE-1), as well as HEK-293T, were purchased from the American Type Culture Collection. RWPE-1, LNCap, 22Rv1, and PC-3 cells were cultured in RPMI-1640 (Gibco), and DU145 and HEK-293T cells were cultured in DMEM (Gibco). All media were supplemented with 10% FBS (Gibco) and 1% penicillin/streptomycin (Gibco). Cells were grown in a humidified atmosphere of 5% CO_2 at 37°C.

2.3 | RNA extraction and qRT–PCR

For total RNA extraction, cells were harvested and isolated with an RNA-Quick Purification Kit (YiShan Biotech) following the standard protocol. Complementary DNA (cDNA) was generated with the PrimeScript RT Reagent Kit (Takara) and analyzed through quantitative real-time PCR (qRT–PCR) with TB Green Premix Ex Taq II (Takara) according to the protocol. GAPDH was used as a loading control. The primer sequences used in this study are listed in Table S1.

2.4 | Animal experiments

Subcutaneous xenograft models were generated as previously described.[10] First, 5×10^6 PC-3 cells with circARHGEF28 stable overexpression were subcutaneously injected into mice (Balb/c nu/nu mice, male, 4 weeks old, 5 mice were blindly and randomly divided into groups). The volumes of tumors were recorded 1 week after injection. All mice were sacrificed after 26 days to obtain subcutaneous tumors. Samples were fixed in 37% formalin and embedded in paraffin for subsequent histological analysis. All the sample weights and volumes were recorded by another experimenter who was unaware of the experimental groups.

2.5 | HE and immunohistochemistry

Tissues were fixed with formalin and then embedded in paraffin after animal sacrifice. For HE staining, hematoxylin (stained nucleus) and eosin (stained cytoplasm) were used. For the immunohistochemistry (IHC) assay, the primary antibody and secondary antibody were as follows: anti-Ki-67, 1:2000 (Cat. No. ab15580; Abcam), goat anti-rabbit IgG, 1:500 (Cat. No. ab6721; Abcam). All images were captured by a Leica DM2000 microscope (Leica Camera AG). The Ki-67-positive rate was determined by two independent pathologists.

2.6 | Biotin-labeled RNA pull-down and capture assay

Biotin-labeled probes for circARHGEF28 or NC and biotinylated biotin-labeled miR-671-5p or negative control (NC) were synthesized by GenePharma. All the information about the probe and primer is listed in Tables S1 and S2. For RNA pull-down, streptavidin magnetic beads (Thermo) were washed with lysis buffer rotated with probe to form probe-coated beads (25°C for 2 h) and then incubated with cell (1×10^7) lysate overnight at 4°C. TRIzol (Invitrogen) was used to extract RNA. After synthesizing cDNA as described above, qRT–PCR was performed for analysis. For the capture assay, cells were seeded and cultured to approximately 70% density and then transfected with biotin-labeled miR-671-5p mimics. After culturing for 48 h, the cells were harvested, lysed, and rotated with streptavidin magnetic beads overnight at 4°C. RNA was isolated and analyzed according to the protocol described above.

2.7 | Oligonucleotide transfection

Small interfering RNA (siRNA), miRNA mimics, and corresponding negative control oligos were synthesized and purchased from GenePharma. Detailed sequence information is listed in Table S3. Cells were seeded and cultured in six-well plates at 50%–70% density, and transfection was performed by Lipofectamine RNAiMax (Invitrogen) according to the protocol. After culturing for indicated times, cells were harvested for subsequent assays. siRNA information is listed in Table S3.

2.8 | Dual-luciferase reports assay

HEK-293T cells (8×10^4) were seeded in 96-well plates and cultured. Luciferase reporter plasmids (psi-CHECK2) containing binding sites were constructed (IGE BIO) and cotransfected with miR-671-5p mimics using Lipofectamine 3000 reagent. Luciferase activity was measured using a dual luciferase assay kit (Promega) according to the protocol after 48 h of transfection. Renilla and firefly luciferase (Rluc) intensity was measured using a SPARK 10 M spectrophotometer (Tecan).

2.9 | Statistics

Statistical analyses were performed using GraphPad Prism 7.0 (GraphPad). All experiments were performed in triplicate, and the results are presented as the means ± SD. Two-tailed Student's *t*-test and one- or two-way analysis of variance were used to analyze statistical significance as appropriate for comparing two groups or multiple groups. $P<0.05$ was considered statistically significant.

2.10 | Additional methods

CCK-8, colony formation, Transwell, RNase R treatment, actinomycin D assays, nuclear-cytoplasmic fractionation and fluorescence in situ hybridization (FISH), plasmid construction, extraction and transfection, flow cytometry, western blot, and bioinformatics analysis are described in Appendix S1.

3 | RESULTS

3.1 | Identification and characteristics of circARHGEF28 in PCa cells

CircARHGEF28 is considered to be a crucial tumor-related molecule.[18] To explore the function of circARHGEF28 in PCa, the expression of circARHGEF28 in PCa cells and tissues was analyzed and downregulation of circARHGEF28 in PCa was observed (Figures 1A,B and S1A), indicating that circARHGEF28 might be negatively associated with PCa progression. To confirm this molecule is circRNA, we conducted several experiments to identify its characterization. Through the results of qRT–PCR, we found that circARHGEF28 was amplified by random primers rather than oligo primers, and agarose gel electrophoresis further showed that circARHGEF28 was specifically detected in cDNA rather than in gDNA (Figure 1C,D). Sanger sequencing showed that circARHGEF28 was similar to hsa_circ_0005777 (chr5: 73136304–73,136,585) identified in circBase (http://circrna.org/), indicating that circARHGEF28 was derived from exon 11 of the ARHGEF28 gene (Figure 1E). Previous research suggested that circRNAs show remarkable stability due to the covalently closed loop, and we also found that circARHGEF28 was resistant to actinomycin D; nevertheless, the linear mRNA of ARHGEF28 was notably decreased after actinomycin D treatment (Figure 1F,G). In addition, circARHGEF28 abundance was maintained at a high level even after treatment with RNase R, whereas the linear transcript clearly decreased under the same conditions (Figure 1H). Additionally, subcellular fractionation assay showed that circARHGEF28 was located in the cytoplasm (Figure 1I), which was consistent with the results of FISH (Figure 1J). These results indicate that circARHGEF28 is a circular RNA and downregulated in PCa. The biogenesis of circRNAs is regulated by specifc RNA-binding proteins.[8] Through analysis of circARHGEF28 sequence in CircInteractome and RBPsuite, eIF4A3 was predicted to have potential matching site with flanking regions of circARHGEF28 (Figure S2A,B). Further investigation revealed that eIF4A3 was upregulated in PCa cells and inhibition of eIF4A3 significantly increased circARHGEF28 (Figure S2C–G), suggesting that eIF4A3 mediated circARHGEF28 expression.

3.2 | CircARHGEF28 inhibited proliferation, invasion, and migration in vitro

The biological roles of circARHGEF28 were validated subsequently. We constructed the stable circARHGEF28 overexpression vector for subsequent validation. We found that overexpressing circARHGEF28 significantly blocked PCa cell proliferation and colony formation (Figures 2A,B,E and S3A). Additionally, siRNAs were transfected to knockdown circARHGEF28 for further validation (Figure S3B,C).

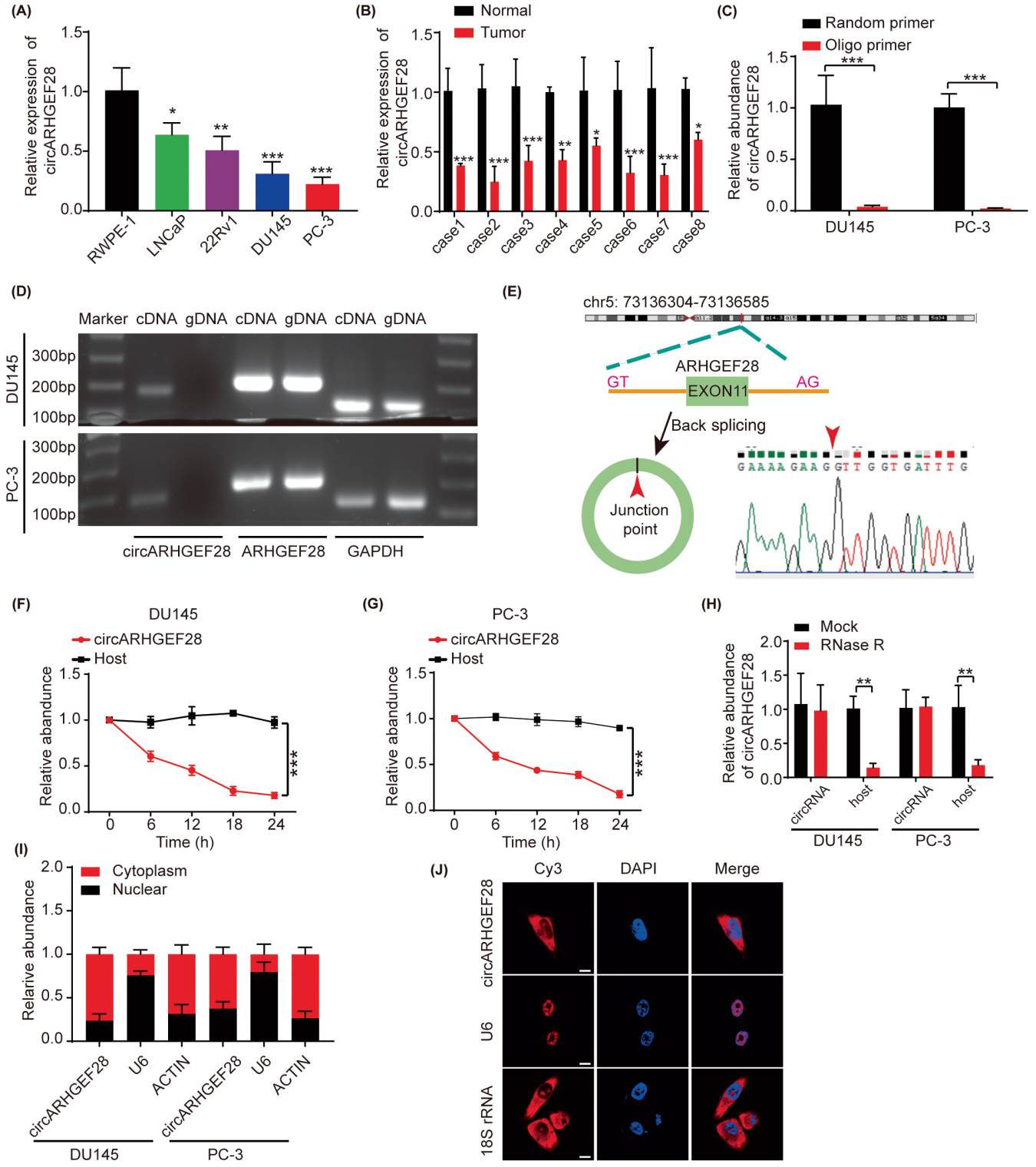

FIGURE 1 The characteristics of circARHGEF28 in PCa cells. (A, B) Low expression of circARHGEF28 in PCa cell lines and tissues. (C) circARHGEF28 was ampliated by random primer in PCa cell lines. (D) Gel electrophoresis of validation for PCR products of circARHGEF28 and linear ARHGEF28 derived from cDNA and gDNA. (E) Schematic illustration showing the formation of circARHGEF28 derived from exon 11 of ARHGEF28, Sanger sequencing indicated the "head-to-tail" splicing sites of circARHGEF28 and marked with red arrows. (F, G) qRT-PCR analysis of the expression of circARHGEF28 and ARHGEF28 linear mRNA in DU145 and PC-3 cells by treating with actinomycin D at the priested times. (H) qRT-PCR analysis of the expression of circARHGEF28 and ARHGEF28 linear mRNA in DU145 and PC-3 cells when treating total RNA with or without RNase R. (I) qRT-PCR analysis of circARHGEF28 distribution in PCa cells. (J) Analysis of FISH for the subcellular location of circARHGEF28 in PCa cells. Scale bar: 20 μm. Data are presented as mean ± SD. $^{*}P < 0.05$, $^{**}P < 0.01$, $^{***}P < 0.001$.

We found that knockdown of circARHGEF28 promoted cell proliferation and colony formation of PCa cells as expected (Figures 2C,D,F and S3D). Importantly, the tumor suppressive function of circARHGEF28 disappeared when the concentration of siRNA solution reached 40 and 80 nM in DU145 and PC-3 cells, respectively (Figure S3E,F). Growth inhibition caused by circARHGEF28 was also observed in RWPE-1 cells (Figure S3G,H). Flow analysis further showed that circARHGEF28 regulated cell apoptosis rather than cell cycle to influence cell proliferation (Figure S4A–D). Migration and invasion are also characteristics in tumor progression. Thus, we next investigated whether circARHGEF28 regulated the migration and invasion of PCa cells. We observed that migration and invasion were dramatically inhibited in the circARHGEF28 overexpression group compared with the empty vector group (Figure 2G,H). Moreover, the invasion and migration capacities of PCa cells were notably enhanced when circARHGEF28 was inhibited (Figure 2I,J). Taken together, these results imply that circARHGEF28 inhibits PCa progression in vitro.

3.3 | CircARHGEF28 suppressed the proliferation of xenograft tumors in vivo

The roles of circARHGEF28 in vivo were also investigated by constructing a mouse xenograft model. PC-3 or 22Rv1 cells with overexpression or knockdown of circARHGEF28 were subcutaneously injected into BALB/c nude mice (Figures 3A and S5A). The results clearly showed circARHGEF28 remarkably inhibited PCa progression in vivo (Figures 3B,C and S5B,C). Moreover, IHC revealed that circARHGEF28 overexpression decreased the number of Ki-67-positive cells (Figure 3D,E), suggesting that circARHGEF28 suppressed the proliferation of PCa cells in vivo. The AR pathway is closely related to PCa[3], therefore we explored the relationship between circARHGEF28 and androgen receptor (AR). It was shown that circARHGEF28 hardly affected the protein level of AR in vitro and in vivo (Figure S5D–F). Analysis of qRT-PCR in vitro also confirmed that circARHGEF28 had little role in regulating AR mRNA (Figure S5G–H). These results indicated that circARHGEF28 promoted PCa progression through an AR-independent pathway.

3.4 | CircARHGEF28 functions as a miRNA sponge for miR-671-5p

Previous studies have reported that circRNAs, located primarily in the cytoplasm, may sponge miRNA to regulate cancer progression by eliminating inhibition of downstream targets. Considering that circARHGEF28 is mainly distributed in the cytoplasm, we speculate that circARHGEF28 may sponge miRNAs to regulate PCa progression. After analyzing miRNA databases (MiRanda, CircInteractome, and RNAhybirdcount), 11 miRNAs (miR-15a-3p, miR-211-5p, miR-759, miR-1225-5p, miR-4455, miR-5581-3p, miR-375, miR-626, miR-671-5p, and miR-889) were predicted (Figure 4A). To accurately identify the potential binding molecule, an RNA pull-down assay was performed. After purification through the biotin-labeled circARHGEF28 probe and oligo probes, qRT–PCR results showed that miR-759, miR-626, and miR-671-5p were specifically highly enriched by the circARHGEF28 probe (Figure 4B,C). To further validate this phenomenon, a dual luciferase vector containing the potential binding sequence of miRNAs was designed and synthesized (Figure 4D) and then we found that only miR-671-5p significantly reduced the Rluc activity of the circARHGEF28 reporter, while there was no significant change in miR-759 and miR-626 (Figure 4E). Moreover, RNA capture assays further confirmed the relationship between circARHGEF28 and miR-671-5p (Figure 4F). In addition, FISH confirmed that circARHGEF28 and miR-671-5p colocalized in the cytoplasm (Figure 4G). Taken together, these results indicate that miR-671-5p might be the binding partner of circARHGEF28.

3.5 | miR-671-5p promoted the proliferation, invasion, and migration of PCa cells in vitro

Although miR-671-5p is a crucial tumor driver,[19,20] the molecular function in PCa was elusive. By analyzing the sequencing data, we found that miR-671-5p was remarkably upregulated in tumor tissues compared with normal epithelial tissues, as well as in metastasis tissues (Figures 5A–C and S6A). Moreover, the expression of miR-671-5p in clinical PCa specimens was dramatically higher than that in normal tissues (Figure 5D). The biological roles of miR-671-5p in PCa cells were investigated subsequently, and we found that inhibition of miR-671-5p significantly suppressed the proliferation of PCa cells compared with the NC (Figure 5E,F) as well as the ability of migration and invasion of PCa cells (Figure 5G,H). Additionally, the mimics of miR-671-5p in DU145 and PC-3 cells displayed a significant enhancement effect regarding cell proliferation (Figure S6B–E). Similarly, migration and invasion also markedly improved under treatment of miR-671-5p mimics (Figure S6F,G). These results indicate that miR-671-5p accelerates proliferation, migration, and invasion of PCa cells.

3.6 | LGALS3BP suppressed the NF-κB pathway and progression of PCa as a target of miR-671-5p

miRNAs regulate the expression of target genes by directly binding to the 3′ UTR of target genes.[21] Therefore, we speculated that miR-671-5p interacts with the 3′ UTR of downstream genes. By analyzing public datasets (mirTarBase, miRWalk, miRDB, TargetScan), five candidate genes (LGALS3BP, DDX39B, BCAP31, CPNE2, HNRNPUL1) were screened (Figure 6A). By analyzing TCGA dataset, we found that LGALS3BP was remarkably decreased in tumor tissues compared with paired normal tissues, with no

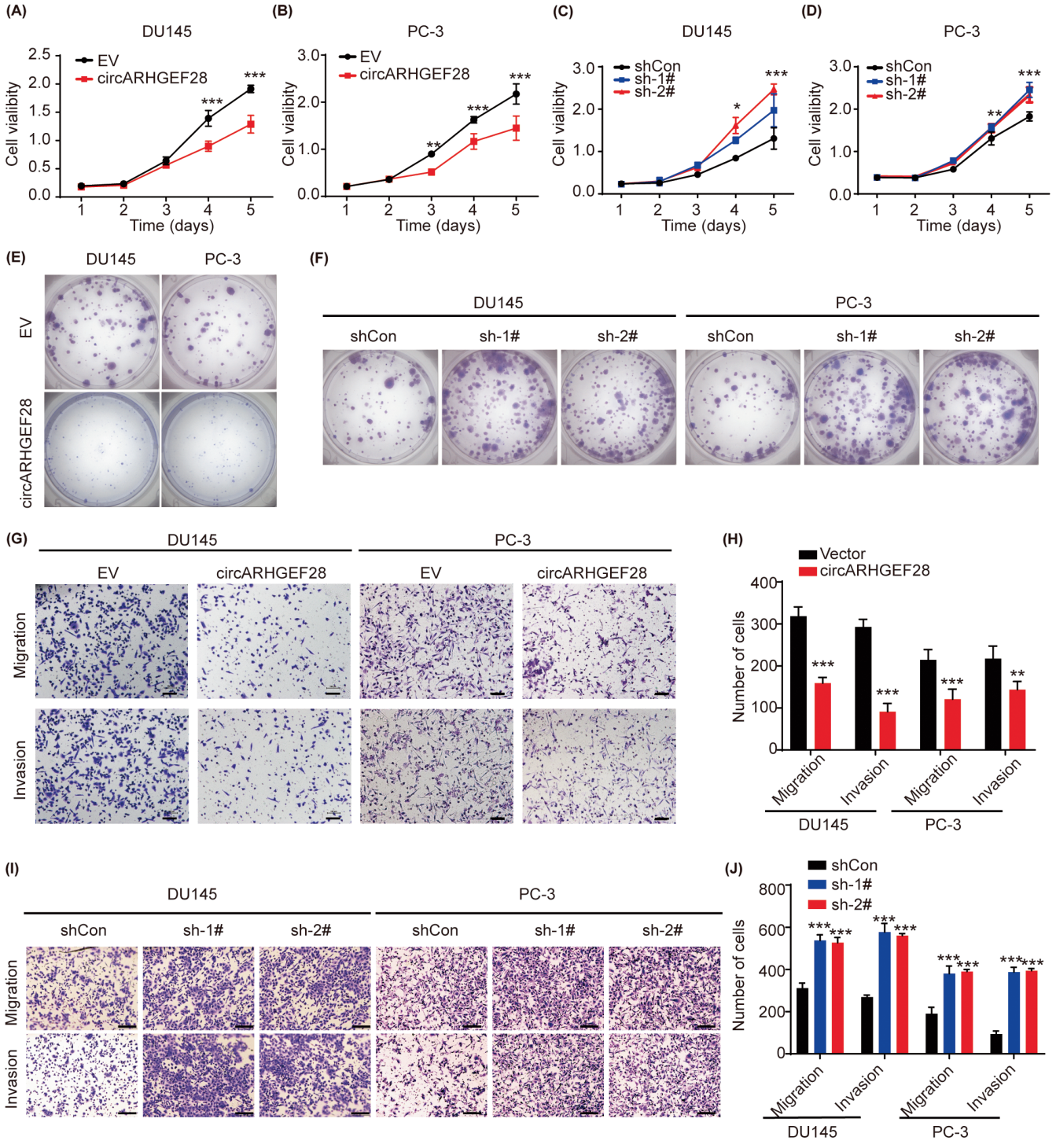

FIGURE 2 circARHGEF28 inhibited the progression of PCa in vitro. (A, B) CCK-8 analysis of cell proliferation of DU145 and PC-3 cells after circARHGEF28 overexpression by transfecting vector. Empty vector (EV) as negative control. (C, D) CCK-8 analysis of cell proliferation of DU145 and PC-3 cells after silencing circARHGEF28 (sh-1#, sh-2#). (E, F) Colony formation assay detected the proliferation of DU145 and PC-3 by circARHGEF28 overexpression (E) or knocking down (F). (G, H) Transwell assay showing the ability of migration and invasion (Matrigel treated) of DU145 and PC-3 by transfecting circARHGEF28 overexpression vector. Scale bar: 200 μm. (I, J) The migration and invasion (Matrigel treated) of DU145 and PC-3 cells were measured by transwell assay after circARHGEF28 knocking down. Scale bar: 100 μm. All the data are presented as mean ± SD. $^{*}P<0.05$, $^{**}P<0.01$, $^{***}P<0.001$.

significant changes in DDX39B, BCAP31, CPNE2, and HNRNPUL1 (Figure 6B), indicating that LGALS3BP was likely associated with PCa progression. Hence, we hypothesized that LGALS3BP might be a potential target of miR-671-5p, and we found that miR-671-5p mimics decreased the expression of LGALS3BP but had no significant regulatory role in DDX39B, BCAP31, CPNE2, or HNRNPUL1 (Figure 6C–E). MiR-671-5p inhibitors significantly increased the expression of LGALS3BP mRNA, as well as the identified target

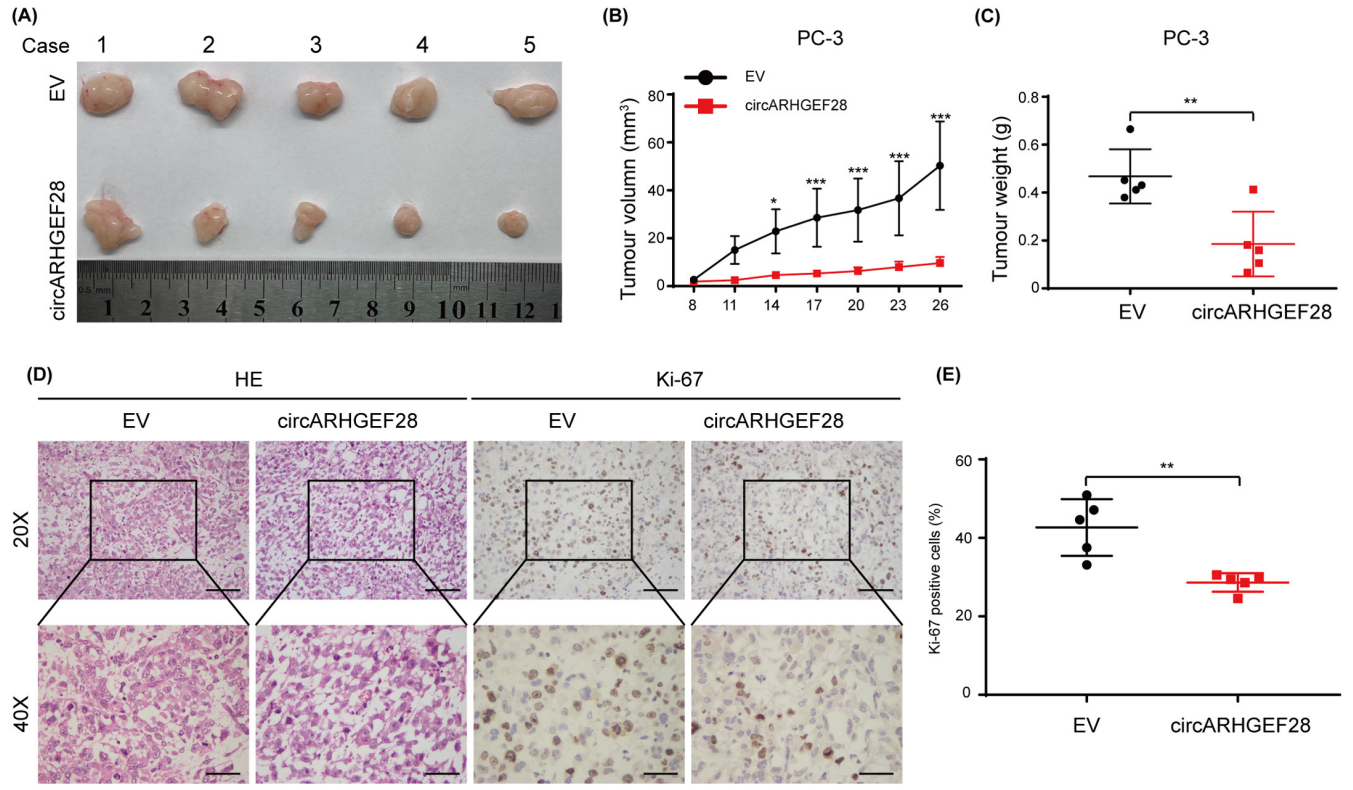

FIGURE 3 circARHGEF28 inhibited the progression of PCa in vivo. (A) Images of subcutaneous xenograft tumors by injecting PC-3 cells with stably overexpressing circARHGEF28 (OE). (B, C) Analysis of tumor volumes and weight for each group (empty vector and OE), $n=5$. (D) Representative images of HE and IHC staining (Ki-67) for subcutaneous xenograft tumors at 200× (scale bar: 100 μm) or 400× (scale bar: 50 μm) magnification. (E) Analysis of Ki-67 expression in subcutaneous xenograft tumors. The data are presented as mean ± SD. $^{*}P<0.05$, $^{**}P<0.01$, $^{***}P<0.001$.

(SOX6)[22] reported in previous research (Figure S7A,B). Importantly, luciferase reporter assays clearly showed that Rluc reporter activity was notably decreased when cells were co-transfected with miR-671-5p mimic and LGALS3BP 3′ UTR-wt vector (Figure 6F). These results showed that LGALS3BP was a novel downstream target of miR-671-5p.

The biological roles of LGALS3BP were subsequently explored. After knocking down LGALS3BP in DU145 and PC-3 cells, the ability of proliferation was notably increased (Figure 6G,H), as well as migration and invasion (Figure 6I,J). Additionally, the precise relationship between miR-671-5p and LGALS3BP in PCa progression was further determined, as shown in Figure S7C,D, and the inhibitory effect of miR-671-5p inhibitor on tumor proliferation was significantly reversed by knocking down LGALS3BP. A similar phenomenon was observed in cell migration and invasion (Figure S7E–H). It has been confirmed that LGALS3BP is closely related to the NF-κB pathway in tumor biology.[23] Hence, we verified this phenomenon in this study. We found that the phosphorylation of p65 increased, as did the phosphorylation of the inhibitor of kappa B kinase (IKK), which suggested activation of the NF-κB pathway (Figure 6K). Importantly, reanalysis of tumor specimens from tumor-bearing mice also confirmed that circARHGEF28 inhibited the expression of phospho-p65 and phospho-IKK (Figure S8A,B). In conclusion, these results indicate that LGALS3BP is a downstream target of miR-671-5p and may inhibit the development of PCa by negatively regulating the NF-κB pathway.

3.7 | miR-671-5p reverses the biological role of circARHGEF28 as a suppressor in vitro

We further investigated whether miR-671-5p partially eliminated the tumor suppressor effect of LGALS3BP. MiR-671-5p mimics and circARHGEF28 vector were individually transfected or cotransfected into PCa cells. We found that miR-671-5p mimics significantly facilitated proliferation and partly abolished circARHGEF28-induced inhibition in PCa cells, suggesting that miR-671-5p could partly impair the inhibition role of circARHGEF28 (Figure 7A,B). Furthermore, the migration and invasion ability of PCa cells was dramatically attenuated when circARHGEF28 was overexpressed, while miR-671-5p overexpression enhanced migration and invasion in circARHGEF28 vector-transduced PCa cells (Figure 7C–E). From these results, it was found that miR-671-5p impaired the circARHGEF28-induced inhibition of PCa. Subsequently, we further explored the relationship between circARHGEF28/miR-671-5p and the NF-κB pathway. We found that activation of the NF-κB pathway induced by miR-671-5p was significantly abolished by the circARHGEF28 vector

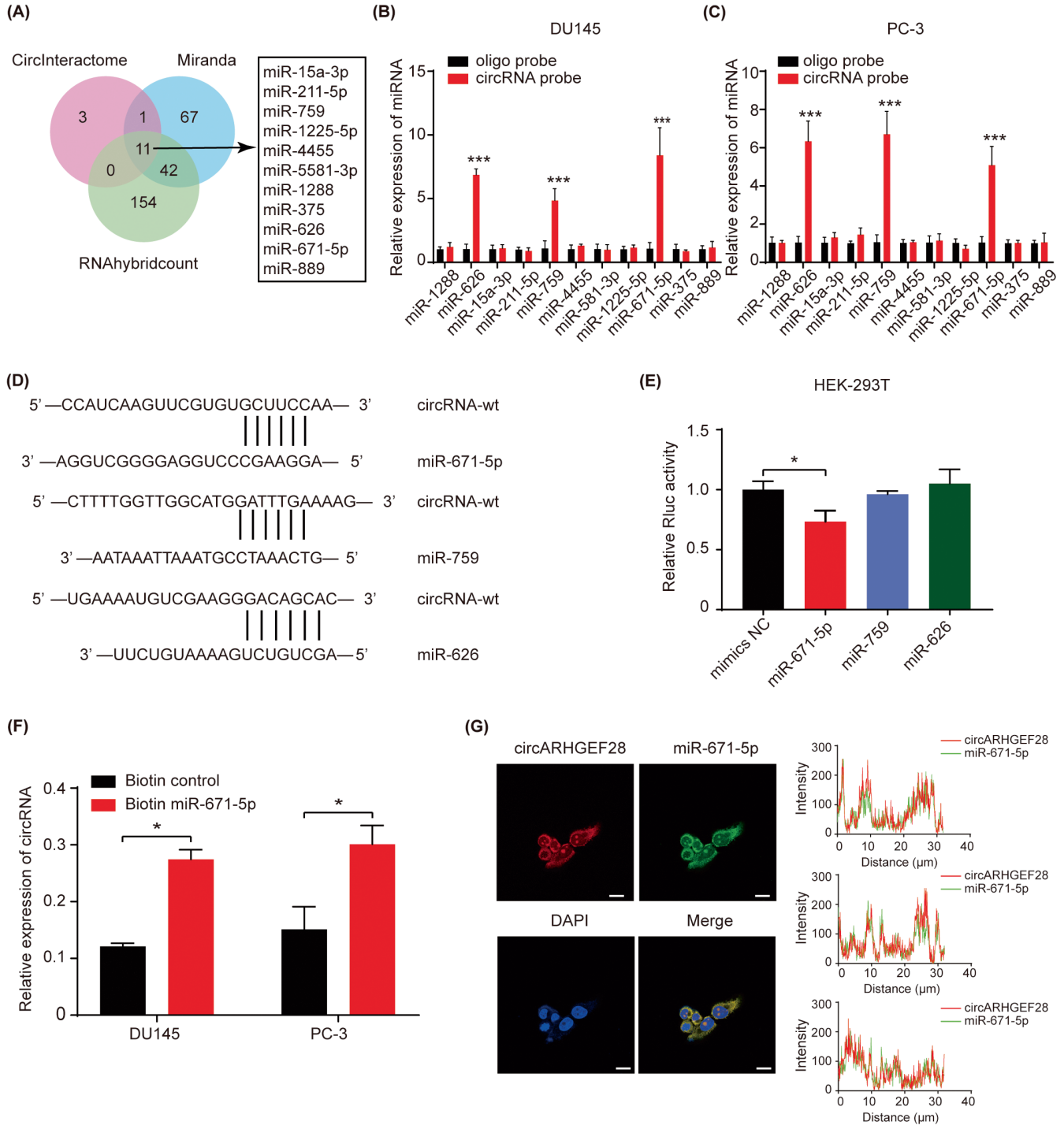

FIGURE 4 circARHGEF28 sponged miR-671-5p in PCa cells. (A) Schematic diagram of binding sites of circARHGEF28 to potential target miRNAs of circARHGEF28 predicted by CircInteractome, Miranda, and RNAhybirdcount. (B, C) RNA pull-down indicated that circARHGEF28 interacted with miR-626, miR-759, and miR-671-5p in DU145 and PC-3. (D) The information of binding site of circARHGEF28 with potential target miRNAs. (E) Dual luciferase reporter assays showing circARHGEF28 combining with miR-671-5p after co-transfecting reporter vector and miR-671-5p mimics in HEK-293T cells. (F) qRT-PCR analysis of abundance of circARHGEF28 after transfecting biotin-labeled miR-671-5p mimics and miRNA capture. (G) Analysis of FISH showing circARHGEF28 co-located in cytoplasm with miR-671-5p in PCa cells. Red fluorescence, Cy3 labeled circARHGEF28 probe; blue fluorescence, FAM labeled miR-671-5p probe. Nuclei were stained with DAPI. Scale bar: 20 μm. The data are presented as mean ± SD. $^{*}P < 0.05$, $^{**}P < 0.01$, $^{***}P < 0.001$.

(Figure 7F). More importantly, we observed a similar trend by examining mRNA changes in the downstream molecules of NF-κB (Figure S8C,D). Taken together, circARHGEF28 functions as an miR-671-5p sponge, further inhibiting activation of the NF-κB pathway, which might be induced by miR-671-5p, thus attenuating the progression of PCa (Figure 7G).

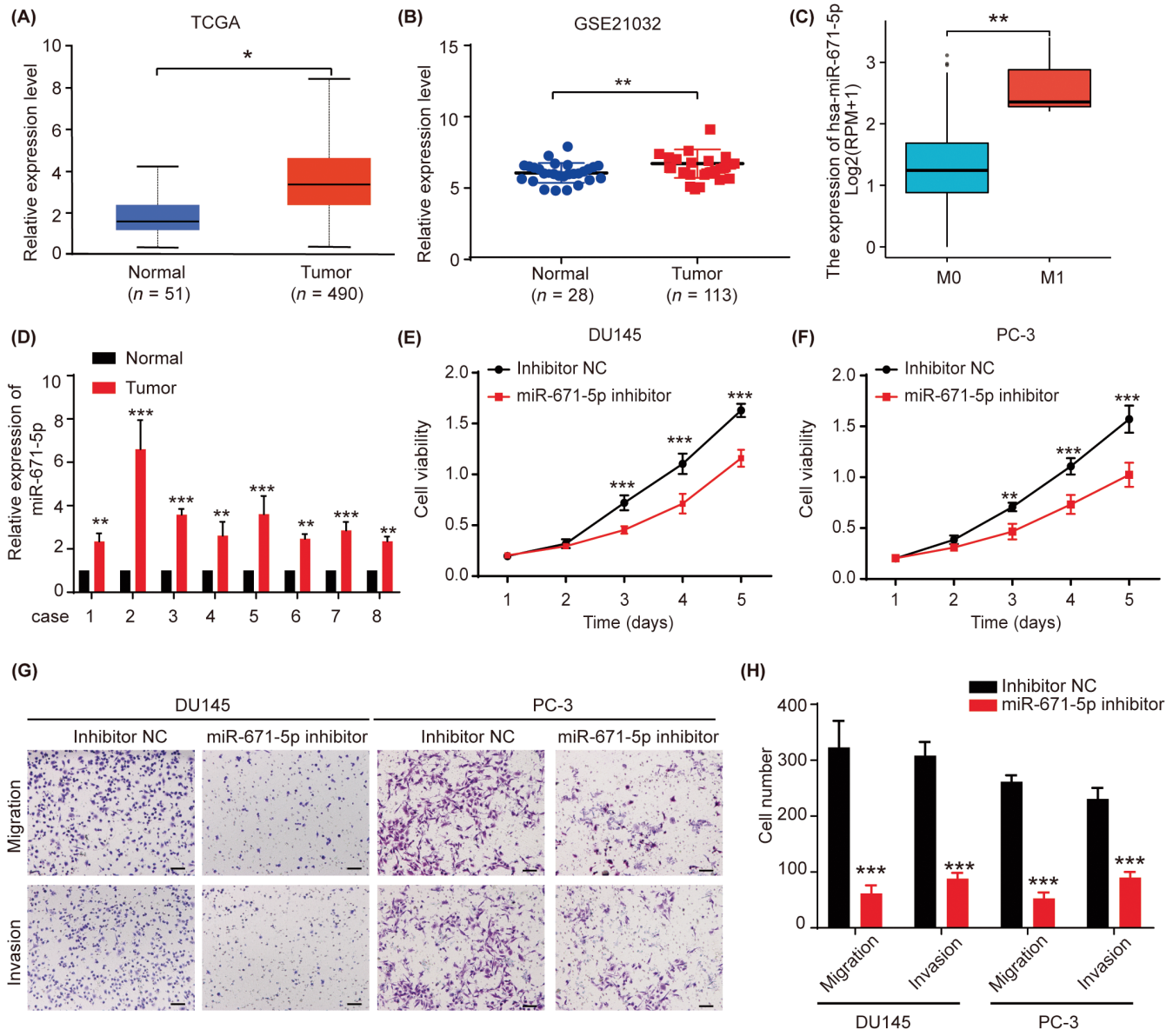

FIGURE 5 miR-671-5p promoted the progression of PCa in vitro. (A–C) The analysis of the expression pattern of miR-671-5p in PCa tissues and metastasis derived from TCGA and GEO datasets (GSE21032). (D) qRT-PCR analysis of expression of miR-671-5p in eight paired PCa tissues. (E, F) Analysis of CCK-8 for measuring proliferation ability in DU145 (E) and PC-3 (F) cells by treating cells with miR-671-5p inhibitor. (G, H) Transwell assay showing the migration and invasion of PCa cells by transfecting miR-671-5p inhibitor. Scale bar: 100 μm. The data are presented as mean ± SD. $^{*}P < 0.05$, $^{**}P < 0.01$, $^{***}P < 0.001$.

4 | DISCUSSION

Although PCa is one of the most prevalent lethal malignant cancers among males, the survival time has been greatly extended in recent years.[18,24] However, once in an advanced stage, the prognosis becomes significantly worse even with various treatments.[2] Hence, it is crucial to clarify the precise molecular mechanisms of PCa progression for the further improvement of treatment approaches. Studies have reported that circRNAs exert diverse functions and are associated with the behaviors of various tumors, including PCa.[10,25–27] However, the exact relationship between circRNAs and PCa remains indefinable. In the present study, we demonstrated that circARHGEF28 was downregulated in PCa. Furthermore, gain- and loss-of approaches showed that circARHGEF28 inhibited the proliferation, migration, and invasion of PCa, and a similar phenomenon was observed in RWPE-1. Mechanistically speaking, we found that circARHGEF28 upregulated LGALS3BP expression by sponging miR-671-5p, thereby further negatively regulating the NF-κB pathway to inhibit the progression of PCa. Taken together, our findings elaborated a novel regulatory network by which an identified circRNA blocked PCa proliferation, migration, and invasion.

CircRNAs represent a novel noncoding RNA and play a crucial role in tumorigenesis and progression of cancers.[28–30] CircRNAs function as miRNA sponges to restore the expression of downstream target of miRNAs, thus regulating the progression of cancers. For instance, circMELK promotes glioblastoma multiforme cell tumorigenesis through

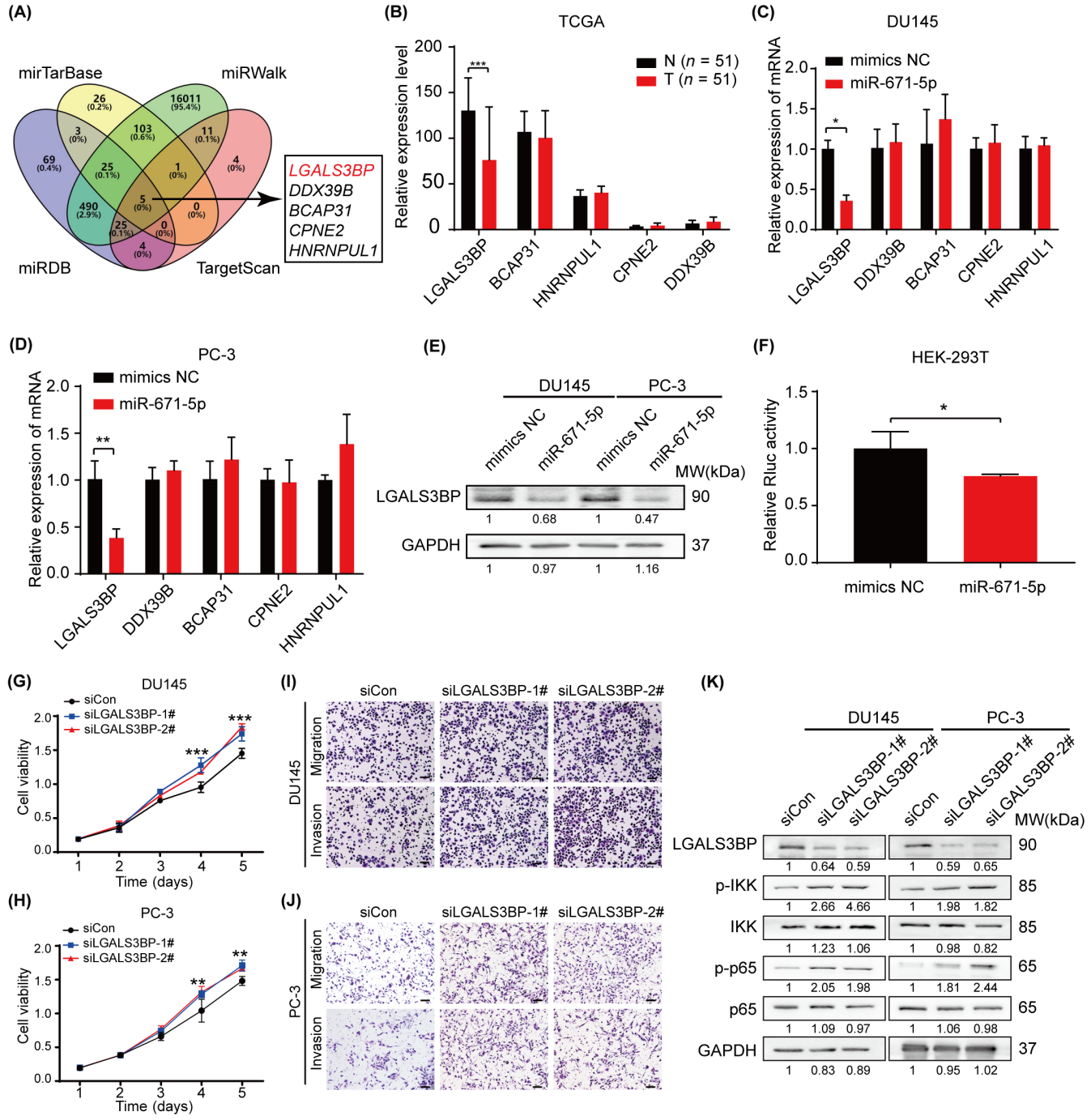

FIGURE 6 LGALS3BP was a target of miR-671-5p and inhibited progression of PCa via the negative regulating NF-κB pathway. (A) Illustration of the candidate target genes of miR-671-5p predicted by mirTarBase, miRWalk, miRDB, and RNAhybirdcount. (B) Analysis of expression of candidate genes in paired PCa tissues derived from TCGA. (C, D) qRT-PCR analysis of potential target genes mRNA by transfecting miR-671-5p mimics in DU145 (C) and PC-3 cells (D). (E) Western blot assay analysis of the protein level of the target gene after transfecting miR-671-5p mimics. (F) Dual luciferase reporter assay showing the relationship between miR-671-5p and LGALS3BP. (G, H) CCK-8 assay showed the proliferation ability of DU145 and PC-3 cells after LGALS3BP was knocked down. (I, J) Transwell assay showed the migration and invasion ability of DU145 and PC-3 cells by transfecting LGALS3BP siRNA duplex. Scale bar: 100 μm. (K) Western blot assay analyzed regulation of NF-κB mediated by LGALS3BP in DU145 and PC-3 cells. GAPDH was used as a loading control. Data are presented as mean ± SD. $^{*}P < 0.05$, $^{**}P < 0.01$, $^{***}P < 0.001$.

miR-593/EphB2 axis.[31] CircSLIT2 facilitates aerobic glycolysis in pancreatic cancer via miR-510-5p/c-Myc/LDHA axis.[32] Importantly, several circRNAs also have been reported to be associated with prognosis of PCa.[33–35] In the present study, we demonstrated that circARHGEF28 colocalized and interacted with miR-671-5p in PCa via endogenous competitive binding. In addition, rescue experiments showed that circARHGEF28 overexpression-induced suppression of colony formation, migration, and invasion could be rescued by

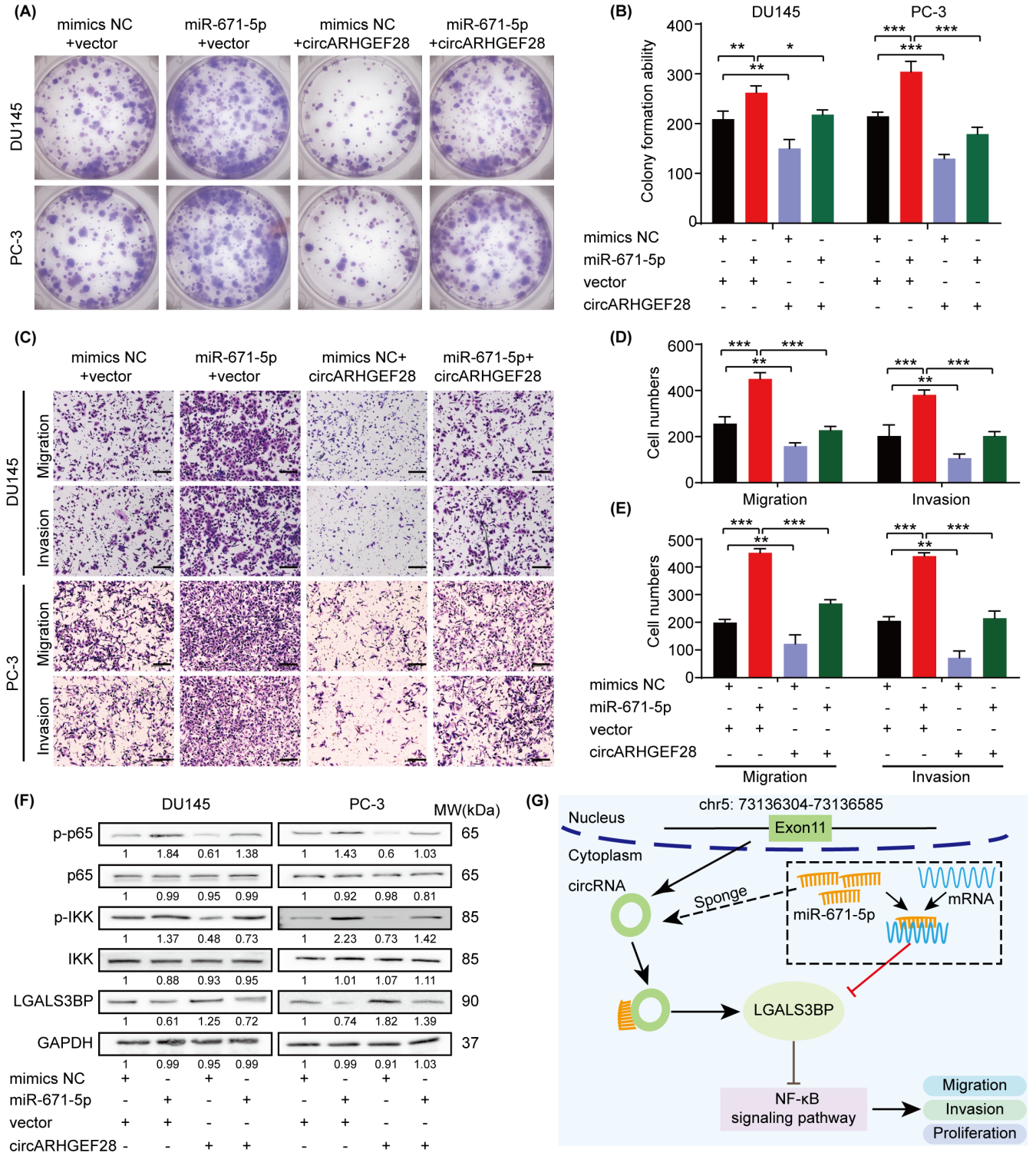

FIGURE 7 miR-671-5p abolished the tumor suppressor of circARHGEF28 in PCa. (A, B) Analysis of colony formation in DU145 and PC-3 cells by transfecting cells with miR-671-5p mimics or mimics NC, circARHGEF28 plasmid or empty vector. (C–E) Analysis of migration and invasion of DU145 and PC-3 by transfecting cells with miR-671-5p mimics or mimics NC, circARHGEF28 plasmid or empty vector. scale Bars: 100 μm. (F) Western blot assay analyzed the regulation of NF-κB mediated by miR-671-5p mimics or mimics NC, transfecting cells with circARHGEF28 plasmid or empty vector. GAPDH was used as a loading control. (G) Schematic illustration showing the regulatory network based on the circARHGEF28/miR-671-5p/LGALS3BP/NF-κB axis. The data are presented as mean ± SD. $^{*}P < 0.05$, $^{**}P < 0.01$, $^{***}P < 0.001$.

upregulating miR-671-5p. Moreover, we also further determined the minimum expression level of circARHGEF28 for its tumor suppressor function, providing a theoretical basis for the subsequent development of ncRNA tumor vaccines using circAHGEF28 as the target. Our findings provide new insight into the ceRNA regulatory network composed of circARHGEF28 and miR-671-5p in PCa.

Although accumulating research has reported that miR-671-5p is a crucial tumor regulator, the precise biological role is contradictory. Zhu et al. found that miRNA-671-5p promotes PCa development by targeting the NFIA/CRYAB axis.[19] However, Song et al. found that miR-671-5p inhibits the development of gastric cancer by devitalizing the PI3K/AKT pathway.[36] Due to organizational dependence, the diverse functions of miR-671-5p in cancers deserves further investigation. In the present study, we found that the expression of miR-671-5p in metastasis tissues was higher than in nonmetastasis tissues. Importantly, miR-671-5p facilitated the proliferation, migration, and invasion of PCa in vitro, indicating the oncogenic role of miR-671-5p in PCa. It is well known that miRNA plays multiple roles via binding to the 3′ UTR of target genes, and SOX6 has been demonstrated to be a target of miR-671.[22] we further confirmed this result in our study, and found that LGALS3BP was another crucial target of miR-671-5p through bioinformatics analysis and dual luciferase experiments, which expanded our knowledge of miR-671-5p.

LGALS3BP is a multifunctional glycoprotein that is involved in diverse biological processes such as inflammation,[37] immune response,[38] and malignant tumors.[39–41] Interestingly, the roles of LGALS3BP in tumors are ambiguous. Several studies report that LGALS3BP functions as a tumor suppressor in colorectal cancer,[42] but a tumor driver in non-small-cell lung cancer and breast cancer.[40,43] Although the downregulation of LGALS3BP in PCa was observed, the precise molecular function is unclear. In the present study, we confirmed that LGALS3BP was downstream of miR-671-5p and discovered that the inhibition of LGALS3BP enhanced the proliferation, migration, and invasion of PCa cells.

Although the biological role of LGALS3BP in PCa was preliminarily revealed, the precise mechanism remains unclear. In the present study, we confirmed that circARHGEF28 was not linked to the AR pathway, but closely to inhibition of the NF-κB pathway. Dysregulation of the NF-κB pathway is frequently observed in various cancers,[44–47] and application of NF-κB inhibitors is a promising strategy.[48] Bortezomib, an inhibitor of the NF-κB pathway, has achieved great success in multiple myeloma[49] and relapsed or refractory mantle cell lymphoma.[50] We not only discovered that miR-671-5p significantly downregulated the expression of LGALS3BP, but also found that downregulated LGALS3BP led to increased p65 phosphorylation and activation of the NF-κB pathway, which is consistent with previous studies.[23,37] Importantly, these results were further confirmed in vivo, thus making our conclusions more plausible. Collectively, our results demonstrate that circARHGEF28 suppresses PCa progression through inactivating the miR-671-5p/LGALS3BP/NF-κB axis, indicating that circARHGEF28 might be a promising therapeutic target in PCa.

ACKNOWLEDGMENTS

This work was supported by the National Natural Science Foundation of China (Grant No. 82072841), the Guangdong Basic and Applied Basic Research Foundation (Grant No. 2021A1515010199), the Science and Technology Program of Guangzhou (Grant No. 201803010029, 202011020004), the Key Areas Research and Development Program of Guangdong (Grant No. 2020B111114002), the Medical Science and Technology Research Foundation of Guangdong Province (Grant No. A2022541), the Guangdong Provincial Clinical Research Center for Urological Diseases (Grant No. 2020B1111170006), the Guangdong Science and Technology Department (Grant No. 2020B1212060018), the Medical Scientific Research Foundation of Guangdong Province (Grant No. C2018060), and the Yixian Clinical Research Project of Sun Yat-sen Memorial Hospital (Grant No. SYS-C-201802).

CONFLICT OF INTEREST STATEMENT

The authors have no conflict of interest.

ETHICS STATEMENT

Approval of the research protocol by an Institutional Review Board: This study was approved by the Ethical Review Committee of Sun Yat-sen Memorial Hospital.

Informed consent: Informed consent was signed before collecting samples.

Registry and the Registration No. of the study/trial: N/A.

Animal studies: Animal experiments were approved by Animal Ethics Committee of Sun Yat-sen University.

ORCID

Kaixuan Guo https://orcid.org/0000-0003-2372-4901
Kewei Xu https://orcid.org/0000-0003-4649-4619

REFERENCES

1. Bray F, Ferlay J, Soerjomataram I, Siegel RL, Torre LA, Jemal A. Global cancer statistics 2018: GLOBOCAN estimates of incidence and mortality worldwide for 36 cancers in 185 countries. *CA Cancer J Clin*. 2018;68:394-424.
2. Teo MY, Rathkopf DE, Kantoff P. Treatment of advanced prostate cancer. *Annu Rev Med*. 2019;70:479-499.
3. Pisano C, Tucci M, Di Stefano RF, et al. Interactions between androgen receptor signaling and other molecular pathways in prostate cancer progression: current and future clinical implications. *Crit Rev Oncol Hematol*. 2021;157:103185.
4. Sartor O, de Bono JS. Metastatic prostate cancer. *N Engl J Med*. 2018;378:645-657.
5. Bill-Axelson A, Holmberg L, Garmo H, et al. Radical prostatectomy or watchful waiting in prostate cancer—29-year follow-up. *N Engl J Med*. 2018;379:2319-2329.
6. Huben RP, Murphy GP. Prostate cancer: an update. *CA Cancer J Clin*. 1986;36:274-292.
7. Kristensen LS, Andersen MS, Stagsted LVW, Ebbesen KK, Hansen TB, Kjems J. The biogenesis, biology and characterization of circular RNAs. *Nat Rev Genet*. 2019;20:675-691.
8. Shen H, Liu B, Xu J, et al. Circular RNAs: characteristics, biogenesis, mechanisms and functions in liver cancer. *J Hematol Oncol*. 2021;14:134.
9. Harper KL, Mottram TJ, Whitehouse A. Insights into the evolving roles of circular RNAs in cancer. *Cancers (Basel)*. 2021;13(16):4180.
10. Shi J, Liu C, Chen C, et al. Circular RNA circMBOAT2 promotes prostate cancer progression via a miR-1271-5p/mTOR axis. *Aging (Albany NY)*. 2020;12:13255-13280.
11. Liu Z, Wang T, She Y, et al. N(6)-methyladenosine-modified circIGF2BP3 inhibits CD8(+) T-cell responses to facilitate tumor immune evasion by promoting the deubiquitination of PD-L1 in non-small cell lung cancer. *Mol Cancer*. 2021;20:105.

12. Xu Y, Zhang S, Liao X, et al. Circular RNA circIKBKB promotes breast cancer bone metastasis through sustaining NF-kappaB/bone remodeling factors signaling. *Mol Cancer*. 2021;20:98.
13. Liu X, Liu Y, Liu Z, et al. CircMYH9 drives colorectal cancer growth by regulating serine metabolism and redox homeostasis in a p53-dependent manner. *Mol Cancer*. 2021;20:114.
14. Yan D, Dong W, He Q, et al. Circular RNA circPICALM sponges miR-1265 to inhibit bladder cancer metastasis and influence FAK phosphorylation. *EBioMedicine*. 2019;48:316-331.
15. Gao X, Xia X, Li F, et al. Circular RNA-encoded oncogenic E-cadherin variant promotes glioblastoma tumorigenicity through activation of EGFR-STAT3 signalling. *Nat Cell Biol*. 2021;23:278-291.
16. Zeng Z, Xia L, Fan S, et al. Circular RNA CircMAP3K5 acts as a MicroRNA-22-3p sponge to promote resolution of intimal hyperplasia via TET2-mediated smooth muscle cell differentiation. *Circulation*. 2021;143:354-371.
17. Zang J, Lu D, Xu A. The interaction of circRNAs and RNA binding proteins: an important part of circRNA maintenance and function. *J Neurosci Res*. 2020;98:87-97.
18. Song W, Lee SW, Chung JH, et al. Relationship between robotic-assisted radical prostatectomy and retropubic radical prostatectomy in the learning curve of a single surgeon as a novice in radical prostatectomy: a retrospective cohort study. *Int J Surg*. 2020;81:74-79.
19. Zhu Z, Luo L, Xiang Q, et al. MiRNA-671-5p promotes prostate cancer development and metastasis by targeting NFIA/CRYAB axis. *Cell Death Dis*. 2020;11:949.
20. Jin W, Shi J, Liu M. Overexpression of miR-671-5p indicates a poor prognosis in colon cancer and accelerates proliferation, migration, and invasion of colon cancer cells. *Onco Targets Ther*. 2019;12:6865-6873.
21. Fabian MR, Sonenberg N. The mechanics of miRNA-mediated gene silencing: a look under the hood of miRISC. *Nat Struct Mol Biol*. 2012;19:586-593.
22. Yu Y, Wang Z, Sun D, et al. miR-671 promotes prostate cancer cell proliferation by targeting tumor suppressor SOX6. *Eur J Pharmacol*. 2018;823:65-71.
23. Hong CS, Park MR, Sun EG, et al. Gal-3BP negatively regulates NF-kappaB signaling by inhibiting the activation of TAK1. *Front Immunol*. 2019;10:1760.
24. Moore C. Prostate-specific membrane antigen PET-CT before radical treatment. *Lancet*. 2020;395:1170-1172.
25. Yang Z, Qu CB, Zhang Y, et al. Dysregulation of p53-RBM25-mediated circAMOTL1L biogenesis contributes to prostate cancer progression through the circAMOTL1L-miR-193a-5p-Pcdha pathway. *Oncogene*. 2019;38:2516-2532.
26. Feng Y, Yang Y, Zhao X, et al. Circular RNA circ0005276 promotes the proliferation and migration of prostate cancer cells by interacting with FUS to transcriptionally activate XIAP. *Cell Death Dis*. 2019;10:792.
27. Chen S, Huang V, Xu X, et al. Widespread and functional RNA circularization in localized prostate cancer. *Cell*. 2019;176(831–843):e822.
28. Li J, Sun D, Pu W, Wang J, Peng Y. Circular RNAs in cancer: biogenesis, function, and clinical significance. *Trends Cancer*. 2020;6:319-336.
29. Zhang HD, Jiang LH, Sun DW, Hou JC, Ji ZL. CircRNA: a novel type of biomarker for cancer. *Breast Cancer*. 2018;25:1-7.
30. Kristensen LS, Hansen TB, Veno MT, Kjems J. Circular RNAs in cancer: opportunities and challenges in the field. *Oncogene*. 2018;37:555-565.
31. Zhou F, Wang B, Wang H, et al. circMELK promotes glioblastoma multiforme cell tumorigenesis through the miR-593/EphB2 axis. *Mol Ther Nucleic Acids*. 2021;25:25-36.
32. Guan H, Luo W, Liu Y, Li M. Novel circular RNA circSLIT2 facilitates the aerobic glycolysis of pancreatic ductal adenocarcinoma via miR-510-5p/c-Myc/LDHA axis. *Cell Death Dis*. 2021;12:645.
33. Deng G, Wang R, Sun Y, et al. Targeting androgen receptor (AR) with antiandrogen enzalutamide increases prostate cancer cell invasion yet decreases bladder cancer cell invasion via differentially altering the AR/circRNA-ARC1/miR-125b-2-3p or miR-4736/PPARgamma/MMP-9 signals. *Cell Death Differ*. 2021;28:2145-2159.
34. Luo J, Li Y, Zheng W, et al. Characterization of a prostate- and prostate cancer-specific circular RNA encoded by the androgen receptor gene. *Mol Ther Nucleic Acids*. 2019;18:916-926.
35. Cao S, Ma T, Ungerleider N, et al. Circular RNAs add diversity to androgen receptor isoform repertoire in castration-resistant prostate cancer. *Oncogene*. 2019;38:7060-7072.
36. Song H, Xu Y, Xu T, et al. CircPIP5K1A activates KRT80 and PI3K/AKT pathway to promote gastric cancer development through sponging miR-671-5p. *Biomed Pharmacother*. 2020;126:109941.
37. Cho SH, Shim HJ, Park MR, et al. Lgals3bp suppresses colon inflammation and tumorigenesis through the downregulation of TAK1-NF-kappaB signaling. *Cell Death Discov*. 2021;7:65.
38. Xu G, Xia Z, Deng F, et al. Inducible LGALS3BP/90K activates antiviral innate immune responses by targeting TRAF6 and TRAF3 complex. *PLoS Pathog*. 2019;15:e1008002.
39. Song Y, Wang M, Tong H, et al. Plasma exosomes from endometrial cancer patients contain LGALS3BP to promote endometrial cancer progression. *Oncogene*. 2021;40:633-646.
40. Kimura R, Yoshimaru T, Matsushita Y, et al. The GALNT6LGALS3BP axis promotes breast cancer cell growth. *Int J Oncol*. 2020;56:581-595.
41. Fogeron ML, Muller H, Schade S, et al. LGALS3BP regulates centriole biogenesis and centrosome hypertrophy in cancer cells. *Nat Commun*. 2013;4:1531.
42. Lee JH, Bae JA, Lee JH, et al. Glycoprotein 90K, downregulated in advanced colorectal cancer tissues, interacts with CD9/CD82 and suppresses the Wnt/beta-catenin signal via ISGylation of beta-catenin. *Gut*. 2010;59:907-917.
43. Woo JK, Jang JE, Kang JH, et al. Lectin, Galactoside-binding soluble 3 binding protein promotes 17-N-Allylamino-17-demethoxygelda namycin resistance through PI3K/Akt pathway in lung cancer cell line. *Mol Cancer Ther*. 2017;16:1355-1365.
44. Liu W, Wang H, Bai F, et al. IL-6 promotes metastasis of non-small-cell lung cancer by up-regulating TIM-4 via NF-kappaB. *Cell Prolif*. 2020;53:e12776.
45. Liu B, Sun L, Liu Q, et al. A cytoplasmic NF-kappaB interacting long noncoding RNA blocks IkappaB phosphorylation and suppresses breast cancer metastasis. *Cancer Cell*. 2015;27:370-381.
46. Saha S, Kiran M, Kuscu C, et al. Long noncoding RNA DRAIC inhibits prostate cancer progression by interacting with IKK to inhibit NF-kappaB activation. *Cancer Res*. 2020;80:950-963.
47. Wang D, Yang L, Yu W, et al. Colorectal cancer cell-derived CCL20 recruits regulatory T cells to promote chemoresistance via FOXO1/CEBPB/NF-kappaB signaling. *J Immunother Cancer*. 2019;7:215.
48. Rasmi RR, Sakthivel KM, Guruvayoorappan C. NF-kappaB inhibitors in treatment and prevention of lung cancer. *Biomed Pharmacother*. 2020;130:110569.
49. Scott K, Hayden PJ, Will A, Wheatley K, Coyne I. Bortezomib for the treatment of multiple myeloma. *Cochrane Database Syst Rev*. 2016;4:CD010816.
50. Hambley B, Caimi PF, William BM. Bortezomib for the treatment of mantle cell lymphoma: an update. *Ther Adv Hematol*. 2016;7:196-208.

SUPPORTING INFORMATION

Additional supporting information can be found online in the Supporting Information section at the end of this article.

How to cite this article: Guo K, Shi J, Tang Z, et al. Circular RNA circARHGEF28 inhibited the progression of prostate cancer via the miR-671-5p/LGALS3BP/NF-κB axis. *Cancer Sci*. 2023;114:2907-2919. doi:10.1111/cas.15820